

Miral J. PATEL^{1,2}, Ashish M. KOTHARI², Hasmukh P. KORINGA¹

¹Government Engineering College, Rajkot, Gujarat, India

²Atmiya University, Rajkot, Gujarat, India

A NOVEL APPROACH FOR SEMANTIC SEGMENTATION OF AUTOMATIC ROAD NETWORK EXTRACTIONS FROM REMOTE SENSING IMAGES BY MODIFIED UNET

Accurate and up-to-date road maps are crucial for numerous applications such as urban planning, automatic vehicle navigation systems, and traffic monitoring systems. However, even in the high resolutions remote sensing images, the background and roads look similar due to the occlusion of trees and buildings, and it is difficult to accurately segment the road network from complex background images. In this research paper, an algorithm based on deep learning was proposed to segment road networks from remote sensing images. This semantic segmentation algorithm was developed with a modified UNet. Because of the lower availability of remote sensing images for semantic segmentation, the data augmentation method was used. Initially, the semantic segmentation network was trained by a large number of training samples using traditional UNet architecture. After then, the number of training samples is reduced gradually, and measures the performance of a traditional UNet model. This basic UNet model gives better results in the form of accuracy, IOU, DICE score, and visualization of the image for the 362 training samples. The idea here is to simply extract road data from remote sensing images. As a result, unlike traditional UNet, there is no need for a deeper neural network encoder-decoder structure. Hence, the number of convolutional layers in the modified UNet is lower than that in the standard UNet. Therefore, the complexity of the deep learning architecture and the training time required by the road network model was reduced. The model performance measured by the intersection over union (IOU) was 93.71% and the average segmentation time of a single image was 0.28 sec. The results showed that the modified UNet could efficiently segment road networks from remote sensing images with identical backgrounds. It can be used under various situations.

Keywords: Semantic Segmentation; UNet; Road Network; Extraction; modified UNet.

1. Introduction

Road network infrastructure is the backbone of any country. In recent times many applications need updated road information frequently such as urban planning, and vehicle routing systems. Hence extraction of road surfaces from high-resolution images is highly significant. On the other hand, updating the road network manually is time consuming and tedious job. However, the roads are modeled as a group of intersections and connections among these intersections [1].

With the support of artificial intelligence, image processing, and machine learning, the automatic extraction of roads from remotely sensed images is a cost-effective and successful mode to obtain road information [2 – 5].

Many researchers proposed road extraction algorithms based on various properties of road features. There are two ways to develop a road network detection system, semiautomatic road and automatic road extraction methods [6, 7]. The method was based on traditional road knowledge, such as road geometry, grey level, and direc-

tion of the road were used to extract a road from RS images [8 –10]. For image detection and monitoring, the majority of researchers have focused on mathematical morphology techniques. This method is always used in conjunction with other image segmentation techniques [11, 12]. Anil P N described a three-step method for extracting road networks from RS pictures using active contours [13].

Recently, the majority of techniques for road detection have relied on classification-based methods [5, 14]. The noisy Landsat satellite images are classified using various algorithms, such as support vectors, logistic regression, and neural networks based on multilayer perceptrons [15]. The comparative analysis revealed that while heterogeneous objects like roads and buildings are recognized poorly overall, aerial objects like water and grass are classified nicely in each method. Overall, the best classification quality was achieved using the neural network-based multilayer perceptron method.

Recently due to high processing hardware easily available deep learning-based algorithms are used to detect road networks from remote sensing images. With the

emergence of deep learning the Convolution Neural Networks (CNN) improve the interpretation by learning more discriminative features [16] such as structural features of images.

1.1. State of art

Many researchers focused on the detection of road parameters from remote sensing images. Road surface extraction was done by a single patch-based Convolution Neural Network (CNN) architecture [17]. RoadNet architecture was examined using high-resolution RS images in a complicated urban scenario [14]. The RoadNet architecture was made up of three end-to-end connected CNNs that perform various tasks. CasNet, a new deep model connected cascaded end-to-end CNNs to extract road and centerlines simultaneously [5]. DenseNet model used few parameters and robust characteristics [18]. UNet with combining residual learning units for road image extraction [19]. From all the methods reported by various researchers, it is concluded that the presence of complex environments such as occlusion or shadows of trees and high elevation buildings, sharp turns, junctions of roads, etc. cause the problem of road extraction from remote sensing images. Moreover, training time, the number of samples used for training the model, and hyper parameters selection are also playing a role in various deep learning-based methods. Therefore, automatic and fast extraction of road network from RS images challenging task.

1.2. Objective

The main objective of this work is to extract automatic and fast road surfaces from remote sensing images which have a complex environment. The method discussed in this paper is based on the UNet [20] architecture as it requires fewer numbers of training samples to train the road model. However, the various numbers of training–testing samples are considered to find the optimum number of training samples which has high road detection accuracy in minimum time. Moreover, it also reduces the number of convolution and de-convolution blocks used in the UNet architecture. This will cause fewer memory resources used and have fast extraction of the road network from the RS images as compared to other methods.

The remainder of this paper is organized as follows. Section 2 introduces the road dataset along with the training–testing splitting of the dataset. However, it also presented the details of our Modified UNet architecture and proposed algorithm to train the road detection network including evaluation metrics and performances. Training - testing time comparison and applicability analysis of our proposed method are provided in Section 3. Finally, the conclusion and discussion will be outlined.

2. Materials and methods of research

2.1. Dataset

We choose the publically available Massachusetts Roads Dataset consists of 1634 aerial images of the state of Massachusetts [21]. Each image is 1500×1500 pixels in size, resolution of 1.2 meter/pixel, covering an area of 2.25 square kilometers. Initially, the dataset has a training set of 1208 images, a validation set of 212 images, and a test set of 214 images. Figure 1 represented some samples of remote sensing images and Figure 2 shows the ground truth of these sample images.

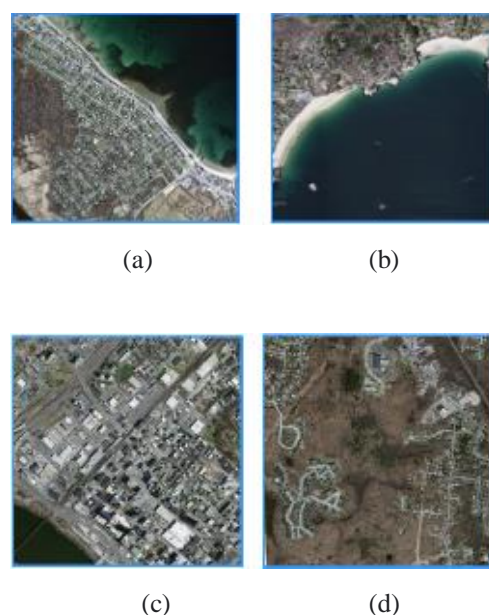


Figure 1. Remote Sensing Original Images:
(a) – image1;(b) – image 2;(c) – image 3;
(d) – image 4

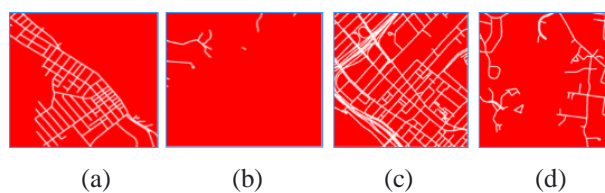


Figure 2. Remote Sensing Ground Truth Images:
(a) – image1;(b) – image 2;(c) – image 3;
(d) – image 4

2.2. Data Augmentation

Initially, the UNet model have been trained by the whole original Massachusetts road dataset. Due to the huge amount of images and big image size needs high training time to train the road segmentation model. So the training sample reduces by half and now it is a total of

604 images. These total images are divided into a training set, validation set, and testing set. Training and testing samples of the dataset are divided into various percentages for evaluation of the road network segmentation model performance as shown in Table 1. Due to less number of training samples used by the model, the data augmentation techniques are used to increase the number of sampled images. The data augmentation [22] on images is done using different techniques such as flipping, cropping, and rotation.

Table 1

Training – Testing Split

Training – Testing split	No of Training images	No of Validation images	No of Testing images
90%-5%	543	30	31
80%-10%	483	60	61
70%-15%	422	91	91
60%-20%	362	121	121
50%-25%	302	151	151
40%-30%	241	182	181
30%-35%	181	212	211

2.3. Modified UNet Road Network System Segmentation Network Structure

For image classification, object detection, and semantic segmentation, convolutional neural networks (CNNs) are beneficial. CNN is the foundation of many well-known networks. These networks are always made up of multiple layers, such as convolutional, pooling, and fully connected layers. By convolving the input of the convolutional layers with a set of filters, feature layers could be obtained. During the training stage, the weights of filters are automatically optimized. The pooling layers combine local picture information and downsample to reduce computational load. CNN has had tremendous success in a variety of fields [23 – 25]. In 2012, Alex Net won the Image Net competition [26]. The Alex Net inspired the development of many CNN-based networks, including inception-v3, GoogleNet, SegNet, VGG, and ResNet [27 – 29]. Because of the ability to the extraction of features these networks are widely used in image processing neural networks. According to previous research, when the number of convolutional layers is increased, the network may extract higher-level image characteristics. Image features extracted are simple when the number of convolutional layers is limited. Here in this paper, binary classification was used to extract road features from the background. So it is not required a deeper neural network for segmentation. The number of computational resources consumed by a neural network can be reduced by simplifying it. In this method, a simple VGG network

was used as the baseline. Figure 3 shows a block diagram for the proposed method for extracting road networks.

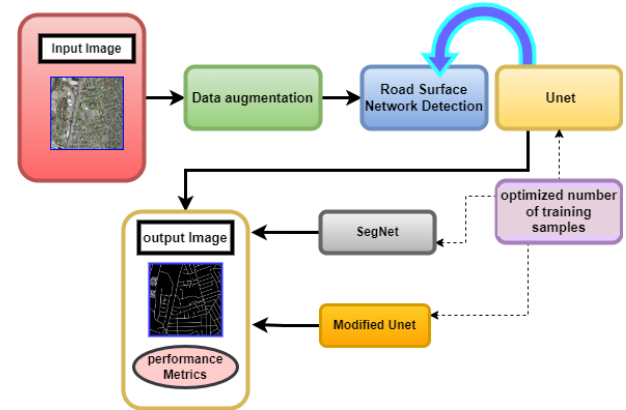


Figure 3. Block diagram for road network extraction system from remote sensing images

The UNet performs very well in semantic segmentation tasks [20]. The detailed architecture of the UNet is described in Figure 4, a. It was originally proposed for biomedical image segmentation. This network is extensively used in image segmentation for two reasons: it is trained from end to end and performs well on a tiny dataset, and the quantity of train samples for UNet is relatively small. UNet is named because of the U shape of its structure. There are two stages: an encoder stage and a decoder stage. The encoding stage is consisting of the convolutional network. It consists of repeated two convolutions; each followed by a rectified linear unit (ReLU) and a max-pooling layer for downsampling. The filter was doubled after each down-sampling step. Every step in the decoder stage comprises a feature map upsampling layer, a concatenation with the corresponding feature map from the encoding stage, and two convolution layers, each followed by a ReLU. A convolution layer is used as the last layer to convert each feature vector to the desired number of classes.

In this paper, the encoder section of UNet and Decoder section of UNet was modified respectively. The four up sample parts of the proposed architecture were reduced to three and the five down sample parts of the proposed architecture were reduced to two. Since binary classification was required to extract road features from the background of the remote sensing images. Therefore, it is not required deeper architecture for semantic segmentation. This architecture was illustrated in the figure by writing the depth of each layer. Due to Less number of convolutional layers reduced the number of hidden layers in the network architecture for modified UNet road segmentation. This causes less number of trainable parameters in the road detection model and saves GPU memory significantly. This will also reduce the training time and segmentation time of a single

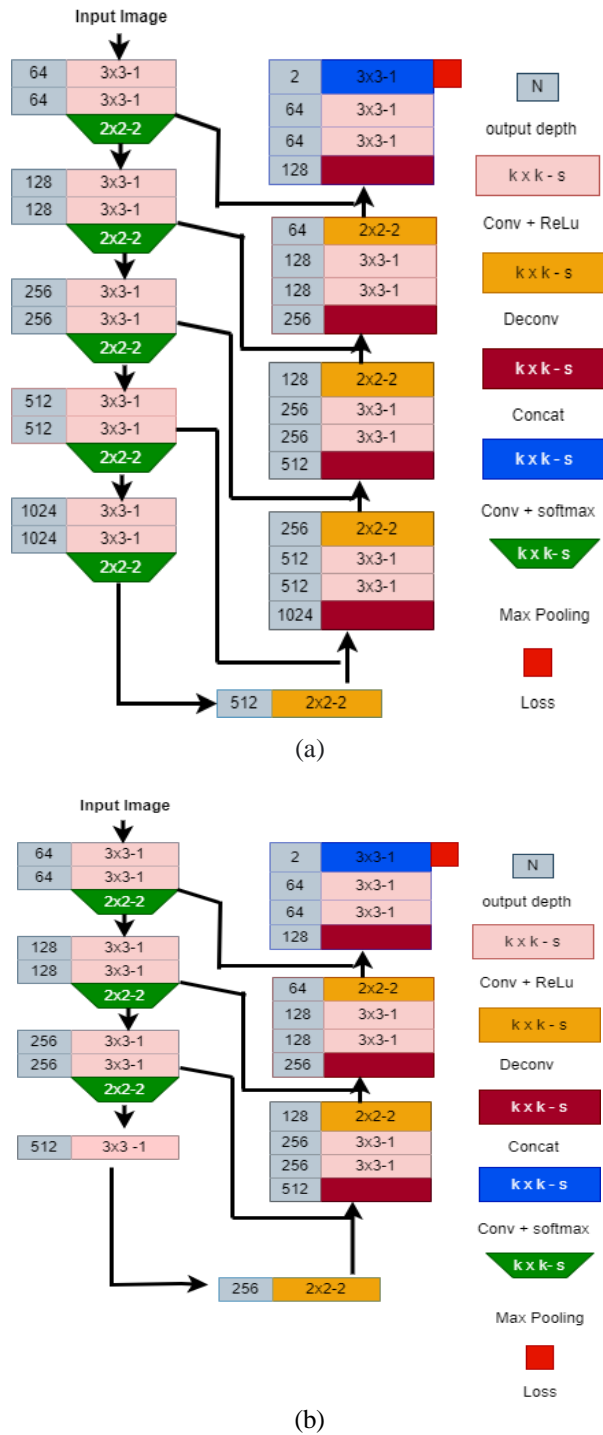


Figure 4. Network Structure:

(a) – UNet Architecture;

(b) – Modified UNet Architecture

remote sensing image. A simplified VGG network was used as the backbone network for encoding. A modified UNet was used as the semantic segmentation network for the extraction of road networks from remote sensing images. The detailed structure of seven convolutional layers together with the max pooling layer and ReLu activation layer at the encoder side of the modified UNet along with the depth and filter size of each layer is

illustrated in Figure 4, b. The decoder is the mirror network of an encoder which also comprises multiple series of concating, deconvolutional, and ReLu activation layers. A sigmoid layer is attached to the last stage of the decoder network to transform the output into probability maps. In this model, to train the road detection network, the cross-entropy loss is utilized, which is defined as

$$L_{bce} = - \sum_{i=1}^b \sum_{j=1}^n GT_{ij} \log(pred_{ij}) + (1 - GT_{ij}) \log(1 - pred_{ij}).$$

Where GT_{ij} is ground truth pixel of i^{th} batch of j^{th} pixel of the image and $pred_{ij}$ is predicted output pixel of i^{th} batch of j^{th} pixel of the image; b is batch size and n = no of the pixel in the images. The sigmoid function is applied to the weighted sums of the hidden layer activations $pred_i$, to generate the outputs of the modified UNet model

$$pred_i = \frac{1}{1 + e^{-\theta_i}},$$

$$\theta_i = \sum_{j=1} w_{ij} h_j.$$

Using the chain rule, we can calculate the error's derivative concerning each weight connecting the hidden and output units

$$\frac{\partial L_{bce}}{\partial w_{ij}} = \frac{\partial L_{bce}}{\partial pred_{ij}} \frac{\partial pred_{ij}}{\partial \theta_{ij}} \frac{\partial \theta_{ij}}{\partial w_{ij}}.$$

2.4. Training of road segmentation Network

The hardware environment used to train the model was Intel (R) Core(TM) i5-7500 K CPU, 8 GB RAM, NVIDIA GeForce RTX 2080 Super. The software environment was Windows 10, CUDA 10.1, Python 3.6, and Tensorflow 2.3. A deep learning algorithm's primary problem is the hyperparameter optimization problem. The research optimizes convolution neural network architecture and finds suitable hyperparameter combinations applied to land cover classification problems using multispectral images [30].

The approach was used to train various architectures for road surface detection, including UNet, SegNet, and modified UNet, as illustrated in Figure 5. However, the Adam optimizer was used to optimize the network. The learning rate was set to 1×10^{-3} . If a larger learning rate was set, the combination of the weights would deviate from the optimal solution, so it was necessary

Algorithm 1: Road Network Extraction System

Input : Training Set = $\{(Y_1, V_1, X_1), \dots, (Y_N, V_N, X_N)\}$
 Where $Y_i=1, \dots, N$ (Training), $V_i=1, \dots, S$ (Validation),
 $X_i=1, \dots, n$ (Testing)
 $Y_N=Y_N^+$
Initialize : Initial Learning Rate α , Batch Size, Epochs T ,
 Initial Loss function $L(v, \theta, t)$

Initialize: $v_1, \theta_1=0, \beta=0.99$
 Build Unet()
 if torch.no_grad() == true; (Training phase)
 start timer():
 for $t=1$ to T do (update parameters)
 $g_t = \nabla \theta f_t(\theta_t - 1)$
 $v_t = \beta(v_{t-1}) + (1 - \beta)g_t^2$
 $\theta_t = \theta_{t-1} - \alpha(m_t / \sqrt{v_t} + \epsilon)$

end for
output: trained θ_t (resulting parameter)
 calculate iou, dice score, accuracy, loss
 if torch.no_grad() != true (validation phase)
 calculate iou, dice score, accuracy, loss
 Plot $T \rightarrow$ accuracy (for training and validation)
 Plot $T \rightarrow$ Loss (for training)
 stop timer():
 if torch.no_grad() != true (testing phase)
 calculate iou, dice score, accuracy;
 import confusion matrix;
 visualize the result

Figure 5. Algorithm for training the module

to reduce the learning rate. The loss function used cross-entropy loss for binary segmentation. The batch size of training was set to 4, hidden layers were set to 64, and epochs were set to 100. During the training process, the loss value, accuracy, dice score, and IOU of the training set and validation set were recorded.

2.5. Road Network segmentation performance evaluation

In this study, four quantitative criteria were used to evaluate the segmentation results. The overall pixel accuracy (Acc), Intersection over Union (IoU), Dice score, and road accuracy were used to assess and compare the segmentation performance (Eqs. (1) – (4)). These parameters are averaged for all the training samples. The Acc, Dice, road accuracy, and IoU were averaged over all images in the testing set. Moreover, the testing time was also measured to assess the segmentation speed of single image and training time was also measured for how long time is required to train the module.

$$iou = \frac{\text{intersection}}{\text{union}},$$

$$iou = \frac{\sum(\text{predi})(GT)}{\sum \text{predi} + \sum GT - \sum(\text{predi})(GT)} 100\%, \dots\dots\dots(1)$$

$$\text{dicescore} = \frac{2 * \text{intersection}}{\text{union} + \text{intersection}},$$

$$\text{dicescore} = 2 * \frac{\sum(\text{predi})(GT)}{\sum \text{predi} + GT} 100\%, \dots\dots\dots(2)$$

$$\text{roadaccuracy} = \frac{\sum TP}{\sum TP + \sum FN} 100\%, \dots\dots\dots(3)$$

$$\begin{aligned} \text{overallaccuracy} &= \\ &= \frac{\sum TP + \sum TN}{\sum TP + \sum TN + \sum FP + \sum FN} 100\%, \dots\dots\dots(4) \end{aligned}$$

where TP is true positive;

TN is true negative;

FP is false positive;

FN is false negative.

3. Results and Discussion

3.1. Result Analysis based on Number of Training Samples and Training Time

Initially, the UNet module was trained with the original Massachusetts publically available dataset. It required a very high amount of training time. Hence the number of training samples was reduced by half to train the UNet model for road network detection. Hence total of 604 training samples was randomly chosen from Massachusetts road data. These images had complex backgrounds such as the occlusion of trees, and cars on road. However, these training samples were divided into training, validation, and testing set. Moreover, we aimed to find an optimized number of training samples that reduced the training time and memory requirement of the model. As a result, the initially trained module employed 90 % of samples for training, 5 % for validation, and the remaining 5 % for testing from 604 images. Successively changed the training sample count from 90 % to 30 % and measured the model's performance metrics by training time as presented in Table 2. Here we considered epoch 30 for finding optimum values of training samples because if trained the model with a large number of the epoch is time consuming and tedious task. Hence the result was compared to the value of epoch 30 by changing the training-testing splitting. As shown in Table 2 the training time is approximate 3.89 hr for 90 % training samples. It gradually decreased as the number of training samples also decreased but the IOU, DICE, and accuracy of the training, validation and testing phase of the model were also decreased as shown in Table 3 and Table 4.

Table 2

Training Time for epoch 30 of different number of Training samples

Training – Testing split	No of the Training images	No of Validation images	No of the Testing images	Training Time(sec)	Training Time (Hr)
90%-5%	543	30	31	14010.86	3.89
80%-10%	483	60	61	13877.64	3.85
70%-15%	422	91	91	11748.96	3.26
60%-20%	362	121	121	5151.07	1.43
50%-25%	302	151	151	4892.18	1.35
40%-30%	241	182	181	4800.2	1.33
30%-35%	181	212	211	4300.3	1.19

Table 3

Training Phase Parameters Comparison when epoch30

Training – Testing split	Training Phase						
	Training				Validation		
	Loss	IOU	DICE	Acc	IOU	DICE	Acc
90%-5%	9.81	79.85	88.37	91.80	87.10	93.05	95.83
80%-10%	8.11	80.10	88.50	92.40	80.66	89.10	93.11
70%-15%	8.87	78.62	87.54	91.32	80.43	88.96	92.47
60%-20%	7.60	79.25	87.97	90.20	79.85	88.55	90.71
50%-25%	5.71	80.39	88.66	91.07	77.33	86.91	88.95
40%-30%	5.84	80.52	88.76	91.08	77.98	87.33	88.87
30%-35%	2.99	82.56	87.79	78.95	78.95	87.96	89.26

Table 4

Testing Phase Parameters Comparison when epoch30

Training – Testing split	Testing			
	IOU	DICE	Overall Accuracy	Road Accuracy
90%-5%	88.59	93.92	95.94	79.27
80%-10%	88.79	94.03	96.19	82.18
70%-15%	85.67	92.12	94.09	80.72
60%-20%	81.87	89.68	91.50	86.93
50%-25%	79.71	88.24	89.54	64.61
40%-30%	79.39	88.04	89.53	0
30%-35%	79.20	87.27	88.72	0.12

Table 5

Approximate the Same Training Time for different epoch

Training – Testing split	Training Time (sec)	Number of Epochs	Testing Phase	
			Overall Accuracy (%)	Road Accuracy (%)
90%-5%	9941.59	20	93.24	70.87
80%-10%	9425.51	22	92.18	69.84
70%-15%	9321.23	23	91.20	68.32
60%-20%	9488.41	60	94.16	91.66
50%-25%	9152.78	62	93.40	87.23
40%-30%	9234.07	70	93.20	74.17
30%-35%	9267.67	71	93.18	70.19

The results of Table 4 indicated road accuracy approximates 0 % for the 40 % and 30 % training samples while highest at the training testing splitting 60 % - 20 % is 86.93 % road pixels were correctly identified. Moreover, the training time for 60 % of training samples was 1.43 hr which was less than half of the 90 % of training samples considered. This yielded the best number of training, validation, and testing samples concerning training time, and the accuracy of the test image was indicated with bold letters in Table 2, Table 3, and Table 4. This result was validated in Table 5 where the model was trained for a similar time but a different number of epochs. The model was tested by testing images and evaluating the performance metrics of overall accuracy and Road accuracy. When considered as 90% of training samples had an epoch of 20 was produced road accuracy was 70.87 % while 30% of trainings amples had an epoch of 71 resulted road accuracy of 70.19 %. However, training samples of 60 % resulted in road accuracy of 91.66 % which is more than 4 % better than 50 % of training samples. However, the designed network is trained on the 1.2 meter /pixel resolution image dataset. So Modified UNet model applies to the resolution of near approximate same but when the remote sensing images have higher resolution it may be required to retrain the model.

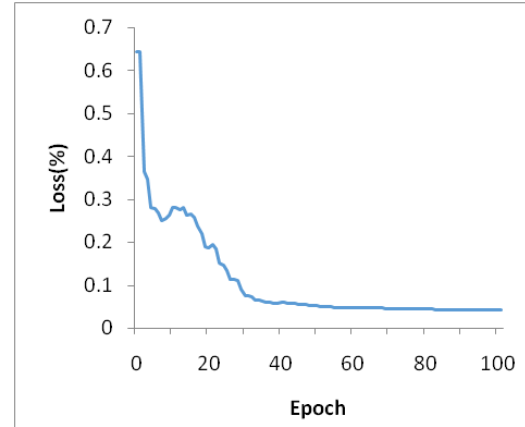
Then after this optimal dataset along with the distribution of samples training-validation-testing splitting is used to train our modified UNet architecture. During the training process of the modified UNet, the loss value and accuracy of each epoch were recorded for the training set and validation set.

Figure 6 shows the process of network training using 60 %-20 % training –testing splitting. It could be seen that with the increase of training epoch, the losses of Modified UNet structure gradually decreased, and the accuracy was gradually increased. There was no overfitting and underfitting. So this number of training samples was enough.

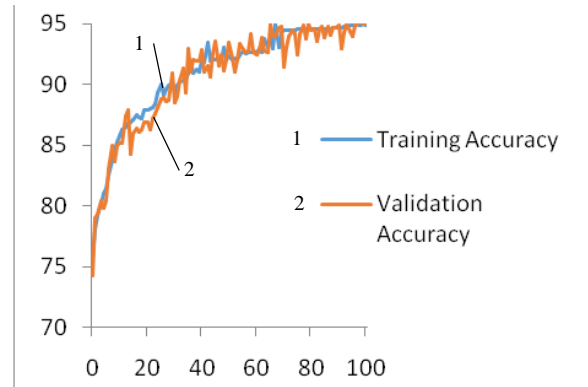
3.2. Comparison with Other Segmentation Method

3.2.1. Training Time and Testing Time Comparison

With the rapid growth of computer hardware in recent years, high-end GPU or GPU clusters have made network training easier. However, given the concern of cost-effectiveness in training time and commercial cost, trade-offs between layer depth, the number of channels, kernel sizes, and other network attributes must still be considered when designing network architectures [31] for experimental research and practical application.



(a)



(b)

Figure 6. Process of Training for modified UNet: (a) – Epoch Vs Loss curve; (b) – Epoch Vs Accuracy for Training and Validation Set

The various evaluation parameters, training time, and inference time were compared to other state-of-the-art deep learning algorithms such as SegNet, and UNet about various numbers of training and testing samples. The SegNet architecture was used as indicated in Figure 7 [32]. It's worth noting that numerous factors, including parameters and model structure, can also affect the running time of deep models, including training and testing time [33]. Figure 8 shows that SegNet has the longest training for all training –testing distribution of any other model. This is due to the deeper structure of SegNet with more Convolutional layers increases the complexity of the model as well as the number of parameters. Moreover, SegNet has the highest inference times compared to any model for all possible training data. The UNet has training and testing time is shorter than SegNet and modified UNet. This is due to the number of convolutional layers being less in the Modified UNet compared to the traditional UNet. Hence less number of learning parameters are required to train the module. Therefore, the least training time and testing time was noted for modified UNet compared to other state of art methods.

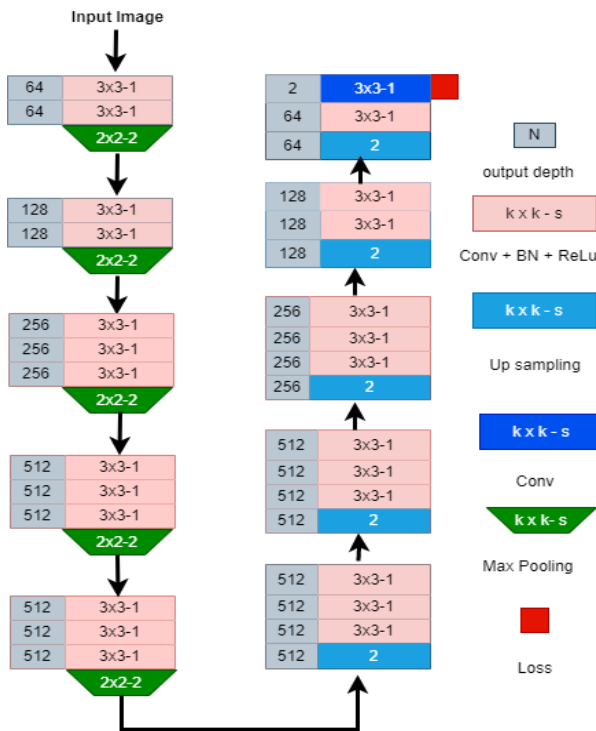
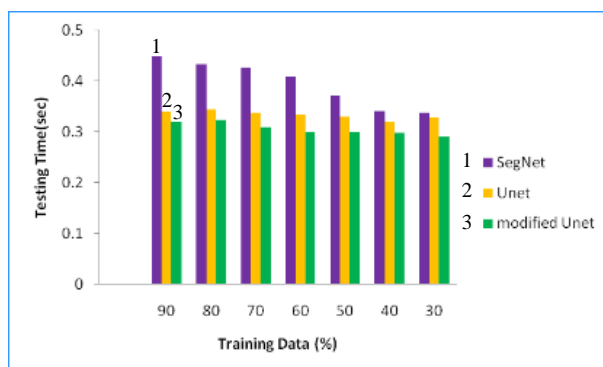


Figure 7. Network Structure SegNet



(a)



(b)

Figure 8. Comparison with other state of art method:
(a) – Training Time; (b) – Testing time

3.2.2. Applicability Analysis of Modified UNet

The SegNet and UNet were constructed by the convolutional neural network. Their segment accuracy was higher. SegNet obtained the details of the result by step-by-step upsampling and convolutional layers. It needs a higher number of training samples. The number of training samples were relatively used small in this paper. Therefore, the performance of this algorithm was not good. Moreover, the optimizer used in SegNet method was SGD which is also one of the reasons for the poor performance of SegNet. To obtain the same accuracy, IOU, and DICE score, SegNet required more number epochs to train the modeled with a lesser number of training samples. So this would be the cause of larger training time and testing time. UNet recovered the details of the result step by step upsampling and merging the features layers from the backbone. Therefore, UNet could segment the details better from the remote sensing images. The target of this image segmentation task was to extract road parts from the remote sensing images. The complexity of the image segmentation task was low. So, the encoding part of the UNet network was simplified according to the characteristics of the low difficulty of the segmentation task.

The last two convolution units (including two convolution layers and one pooling layer) of the VGG network were removed, leaving only the first three convolution units and the two convolution layers in the decoding unit (including one upsampling layer, one concatenate layer, and two convolution layers) were changed into one layer convolution layer. This way the redundant part was removed. Therefore, the simplified network achieved the best segmentation result while the training and testing time was relatively small. The IOU, DICE score, and overall accuracy on the training set were 93.28 %, 93.74 %, and 94.26 % respectively during the training phase of the modified UNet. However, the IOU, DICE score, Overall Accuracy, and Road accuracy have occurred during the testing phase were 92.19 %, 92.68 %, 93.48 %, and 93.3 % respectively (Table 6). Figure 9 depicts the visual result of the various methods.

Conclusion

In this research work initially, road dataset was divided into some Training – Testing splittings and measure the performance of the road detection method. This will determine the optimized number of training samples required to train samples for the deep learning-based model. This same training set was applied to train the module of different types of neural network architecture. Each method applied the data augmentation method to

Table 6

Evaluation of segmentation result with different segmentation methods

Model Name	Training			Testing			
	DICE (%)	IOU (%)	Overall Acc (%)	DICE (%)	IOU (%)	Overall Acc (%)	Road Accuracy (%)
SegNet	93.9	88.74	92.62	91.59	85.18	92.3	91.7
UNet	94.6	93.71	95.1	91.2	87.4	94.2	92.86
Proposed Unet	93.74	93.28	94.26	92.68	92.19	93.48	93.3

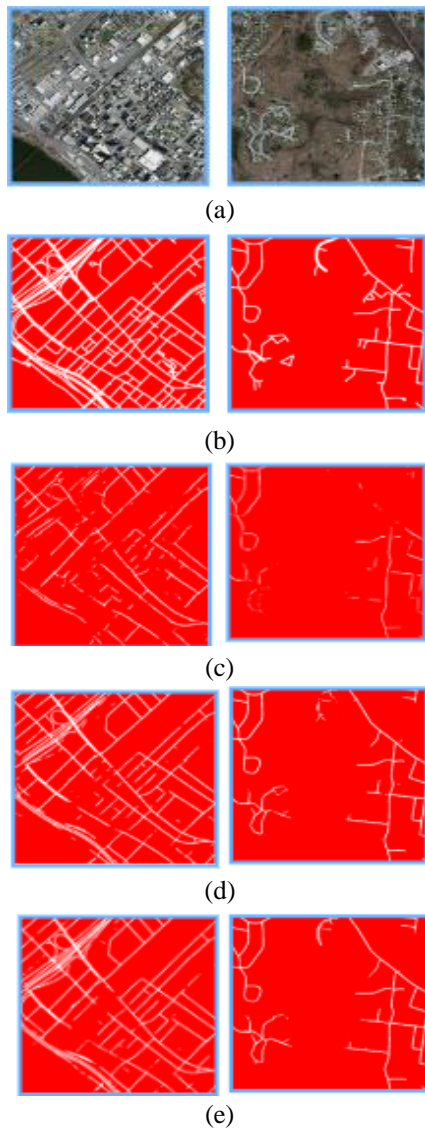


Figure 9. Visual Comparison Of Segmentation Methods:(a) – Original Remote Sensing images; (b) – Ground Truth; (c) – SegNet; (d) – UNet; (e) – Modified UNet

training samples of various semantic segmentation methods. Then, the neural networks were trained for various numbers of epochs to obtain automatic road network segmentation. Through the analysis of the experiment results, it was found that:

1. The modified UNet can effectively segment road images from the remote sensing images. The average value of IoU and Dice score of segmentation occurred at 93.74 %, and 93.28 % respectively during training of the module. During the testing phase, the average value of IOU and DICE scores occurred at 92.19 % and 92.68 % respectively. The training time required for the road network segmentation model was 1.34 hr and the testing time for a single image was 0.3 sec.

2. The dataset could be effectively augmented by the rotate and flip method. This could alleviate the over fitting caused by the lack of training samples.

3. The results showed that the accuracy of the modified UNet was higher than that of other algorithms. And the speed was relatively high.

4. The method of the road network extraction system from the remote sensing images proposed in this paper could accurately segment the road images from the complex background remote sensing images.

The modified UNet proposed in this paper was simplified compared with the basic UNet. The simplified UNet has lower feature extraction and decoding abilities than the original UNet. However, the semantic segmentation task in this paper was a binary classification between the road and background. Only the road and background segments were targeted in this paper. Because of these qualities, the network was simplified, and this simplification diminishes the neural network's capability in complex tasks. However, it improves the accuracy and speed of semantic segmentation of road networks.

Future work

The capability of the road detection networks can be improved with the use of pre-processing and post-processing filters. Furthermore, the learning capacity of the proposed modified UNet architecture can be studied by different optimization techniques.

Contribution of authors: deep learning architecture construction, selection of hyperparameters and optimizer, dataset collection, selection of software tool, simulating and optimizing the model to the minimum amount of training and testing time, analysis of the result, presentation of result, and writing the paper – **Miral J. Patel;**

formulation of conclusion, the content of the paper, review, and analysis of the model and overall review the paper – **Ashish M. Kothari**; analysis of the results, formatting and checking for grammatically of the paper – **Hasmukh P. Koringa**.

All the authors have read and agreed to the published version of the manuscript.

References (GOST 7.1:2006)

1. Multiscale road centerlines extraction from high-resolution aerial imagery [Text] / J. Liu, Q. Miao, J. Song, Y. Quan, Y. Li, P. Xu, J. Dai // *Neurocomputing*. – 2019. – Vol. 329. – P. 384-396. DOI: 10.1016/j.neucom.2018.10.036.2. An end-to-end neural network for road extraction from remote sensing imagery by multiple feature pyramid network [Text] / X. Gao, X. Sun, Y. Zhang, M. Yan, G. Xu, H. Sun, J. Jiao, K. Fu // *IEEE Access*. – 2018. – Vol. 6. – P. 39401-39414. DOI: 10.1109/ACCESS.2018.2856088.
3. Multiscale road extraction in remote sensing images [Text] / A. Wulamu, Z. Shi, D. Zhang, Z. He // *Computational intelligence and neuroscience*. – 2019. – Vol. 2019. – Article ID 2373798. DOI: 10.1155/2019/2373798.
4. Road extraction from remote sensing image based on multi-resolution analysis [Text] / L. Wang, Q. Qin, S. Du, D. Chen, J. Tao // *31th International Symposium on Remote Sensing of Environment*. – 2005. – 4 p.
5. Automatic Road Detection And Centerline Extraction Via Cascaded End-To-End Convolutional Neural Network [Text] / G. Cheng, Y. Wang, S. Xu, H. Wang, S. Xiang, C. Pan // *IEEE Transactions on Geoscience and Remote Sensing*. – 2017. – Vol. 55, no. 6. – P. 3322-3337. DOI: 10.1109/TGRS.2017.2669341.
6. Hormese, J. Automated Road Extraction From High Resolution Satellite Images [Text] / J. Hormese, C. Saravanan // *Procedia Technology*. – 2016. – Vol. 24. – P. 1460-1467. DOI: 10.1016/j.protcy.2016.05.180.
7. A Review Of Road Extraction From Remote Sensing Images [Text] / W. Wang, N. Yang, Y. Zhang, F. Wang, T. Cao, P. Eklund // *Journal Traffic Transp. Eng.* – 2016. – Vol. 3, iss. 3. – P. 271-282. DOI: 10.1016/j.jtte.2016.05.005.
8. Vincent, L. Watersheds In Digital spaces: An Efficient Algorithm Based On Immersion simulation [Text] / L. Vincent, P. Soille // *IEEE Trans. On Pattern Analysis And Machine Intelligence*. – 1991. – Vol. 13, iss. 6. – P. 583-598. DOI: 10.1109/34.87344.
9. Wang, D. A Multiscale Gradient Algorithm For Image Segmentation Using Watersheds [Text] / D. Wang // *Pattern Recognition*. – 1997. – Vol. 30, iss. 12. – P. 2043-2052. DOI: 10.1016/S0031-3203(97)00015-0.
10. Knowledge-Based Road Extraction From High Resolution Remotely Sensed Imagery [Text] / J. Shen, X. Lin, Y. Shi, C. Wong // *IEEE Congress on Image and Signal Processing*. – 2008. – P. 608-612. DOI: 10.1109/CISP.2008.519.
11. Bakhtiari, H. R. R. Semi Automatic Road Extraction From Digital Images [Text] / H. R. R. Bakhtiari, A. Abdollahi, H. Rezaeian // *The Egypt. J. Remote Sensing and Space Science*. – 2017. – Vol. 20, iss. 1. – P. 117-123. DOI: 10.1016/j.ejrs.2017.03.001.
12. Xu, G. Road Extraction In High Resolution Images From Google Earth [Text] / G. Xu, D. Zhang, X. Li // *7th International Conference on Information, Communications and Signal Processing, China, 2009*. – P. 1-5. DOI: 10.1109/ICICS.2009.5397470.
13. Anil, P. N. A Novel Approach Using Active Contour Model For Semi-Automatic Road Extraction From High Resolution Satellite Imagery [Text] / P. N. Anil, S. Natarajan // *Second International Conference On Machine Learning And Computing, 2010*. – P. 263-266. DOI: 10.1109/ICMLC.2010.36.
14. RoadNet: Learning To Comprehensively Analyze Road Networks In Complex Urban Scenes From High-Resolution Remotely Sensed Images [Text] / Y. Liu, J. Yao, X. Lu, M. Xia, X. Wang, Y. Liu // *IEEE Trans. Geosci. Remote Sens.* – 2019. – Vol. 57, no. 4. – P. 2043-2056. DOI: 10.1109/TGRS.2018.2870871.
15. Lukin, V. Comparison of Algorithms for Controlled Pixel-By-Pixel Classification of Noisy Multichannel Images [Text] / V. Lukin, G. Proskura, I. Vasilieva // *Radioelectronic And Computer Systems*. – 2019. – No. 4. – P. 39-46. DOI: 10.32620/reks.2019.4.04.
16. Road And Tunnel Extraction From SPOT Satellite Images Using Neural Networks [Text] / N. Ghasemloo, M. R. Mobasheri, A. M. Zare, M. M. Eftekhari // *Journal of Geographic Information System*. – 2013. – Vol. 5, iss. 1. – P. 69-74. DOI: 10.4236/jgis.2013.51007.
17. Simultaneous Extraction Of Roads And Buildings In Remote Sensing Imagery With Convolutional Neural Networks [Text] / R. Alshehhi, P. R. Marpu, W. L. Woon, M. D. Mura // *ISPRS Journal of Photogrammetry And Remote Sensing*. – 2017. – Vol. 130. – P. 139-149. DOI: 10.1016/j.isprsjprs.2017.05.002.
18. Road Extraction of High-Resolution Remote Sensing Images Derived From DenseUNet [Text] / J. Xin, X. Zhang, Z. Zhang, W. Fang // *Remote Sensing*. – 2019. – Vol. 11, iss. 21. – Article no. 2499. DOI: 10.3390/rs11212499.
19. Zhang, Z. Road Extraction By Deep Residual UNet [Text] / Z. Zhang, Q. Liu, Y. Wang // *IEEE Geosci. Remote Sens. Lett.* – 2018. – Vol. 15, no. 5. – P. 749-753. DOI: 10.48550/arXiv.1711.10684.

20. Ronneberger, O. UNet: Convolutional networks for biomedical image segmentation [Text] / O. Ronneberger, P. Fischer, T. Brox // *Computer Vision and Pattern Recognition*. – 2015. – P. 1-8. DOI: 10.48550/arXiv.1505.04597.

21. Massachusetts dataset [Electronic resource]. – Available at: https://www.cs.toronto.edu/~vmnih/data/mass_roads/train/sat/index.html. – July 2021.

22. Shorten, C. C. A Survey on Image Data Augmentation for Deep Learning [Text] / C. C. Shorten, M. T. Khoshgoftaar // *Journal Big Data*. – 2019. – Vol. 6. – Article No. 60. DOI: 10.1186/s40537-019-0197-0.

23. Jiang, Y. Research on road extraction of remote sensing image based on convolutional neural network [Text] / Y. Jiang // *EURASIP Journal on Image and Video Processing*. – 2019. – Article No. 31. DOI: 10.1186/s13640-019-0426-7.

24. Barbedo, J. G. A. Impact of dataset size and variety on the effectiveness of deep learning and transfer learning for plant disease classification [Text] / J. G. A. Barbedo // *Computers and Electronics in Agriculture*. – 2018. – Vol. 153. – P. 46-53. DOI: 10.1016/j.compag.2018.08.013.

25. Yadav, S. Deep convolutional neural network based medical image classification for disease diagnosis [Text] / S. Yadav, S. M. Jadhav // *Journal of Big Data*. – 2019. – Vol. 6. – Article No. 113. DOI: 10.1186/s40537-019-0276-2.

26. Krizhevsky, A. ImageNet Classification with Deep Convolutional Neural Networks [Text] / A. Krizhevsky, I. Sutskever, G. E. Hinton // *Communications of the ACM*. – 2017. – Vol. 60, iss. 6. – P. 84-90. DOI: 10.1145/3065386.

27. Rethinking the Inception Architecture for Computer Vision [Text] / C. Szegedy, V. Vanhoucke, J. Ioffe, J. Shlens, Z. Wojna // *Computer Vision and Pattern Recognition*. – 2015. – P. 1-10. DOI: 10.48550/arXiv.1512.00567.

28. Going Deeper with Convolutions [Text] / C. Szegedy, W. Liu, Y. Jia, P. Sermanet, S. Reed, D. Anguelov, D. Erhan, V. Vanhoucke, A. Rabinovich // *IEEE Conference on Computer Vision and Pattern Recognition (CVPR)*. – 2015. – P. 1-9. DOI: 10.1109/CVPR.2015.7298594.

29. Deep Residual Learning for Image Recognition [Text] / K. He, X. Zhang, S. Ren, J. Sun // *Computer Vision and Pattern Recognition*. – 2015. – P. 1-12. DOI: 10.48550/arXiv.1409.4842.

30. Yaloveha, V. Convolutional neural network hyperparameter optimization applied to land cover classification [Text] / V. Yaloveha, A. Podorozhniak, H. Kuchuk // *Radioelectronic and computer systems*. – 2022. – No. 1. – P. 115-128. DOI: 10.32620/reks.2022.1.09.

31. He, K. Convolutional neural networks at constrained time cost [Text] / K. He, J. Sun // *IEEE Conference on Computer Vision and Pattern Recognition*. – 2015. – P. 5353-5360. DOI: 10.1109/CVPR.2015.7299173.

32. Badrinarayanan, V. SegNet: A Deep Convolutional Encoder-Decoder Architecture for Image Segmentation [Text] / V. Badrinarayanan, A. Kendall, R. Cipolla // *IEEE Transactions on Pattern Analysis and Machine Intelligence*. – 2017. – Vol. 39, iss. 12. – P. 2481-2495. DOI: 10.1109/TPAMI.2016.2644615.

33. Canziani, A. An Analysis of Deep Neural Network Models for Practical Applications [Text] / A. Canziani, A. Paszke, E. Culurciello // *Computer Vision and Pattern Recognition*. – 2016. – P. 1-7. DOI: 10.48550/arXiv.1605.07678.

References (BSI)

1. Liu, J., Miao, Q., Song, J., Quan, Y., Li, Y., Xu, P., Dai, J. Multiscale road centerlines extraction from high-resolution aerial imagery. *Neurocomputing*, 2019, vol. 329, pp. 384-396. DOI:10.1016/j.neucom.2018.10.036.2. Gao, X., Sun, X., Zhang, Y., Yan, M., Xu, G., Sun, H., Jiao, J., Fu, K. An end-to-end neural network for road extraction from remote sensing imagery by multiple feature pyramid network. *IEEE Access*, 2018, vol. 6, pp. 39401-39414. DOI: 10.1109/ACCESS.2018.2856088.

3. Wulamu, A., Shi, Z., Zhang, D., He, Z. Multiscale road extraction in remote sensing images. *Computational intelligence and neuroscience*, 2019, vol. 2019, article id 2373798. DOI: 10.1155/2019/2373798.

4. Wang, L., Qin, Q., Du, S., Chen, D., Tao, J. Road extraction from remote sensing image based on multi-resolution analysis. *31th International Symposium on Remote Sensing of Environment*, 2005. 4 p.

5. Cheng, G., Wang, Y., Xu, S., Wang, H., Xiang, S., Pan, C. Automatic Road Detection And Centerline Extraction Via Cascaded End-To-End Convolutional Neural Network. *IEEE Transactions on Geoscience and Remote Sensing*, 2017, vol. 55, no. 6, pp. 3322-3337. DOI: 10.1109/TGRS.2017.2669341.

6. Hormese, J., Saravanan, C. Automated Road Extraction From High Resolution Satellite Images. *Procedia Technology*, 2016, vol. 24, pp. 1460-1467. DOI: 10.1016/j.protcy.2016.05.180.

7. Wang, W., Yang, N., Zhang, Y., Wang, F., Cao, T., Eklund, P. A Review of Road Extraction from Remote Sensing Images. *J. Traffic Transp. Eng.*, 2016, vol. 3, iss. 3, pp. 271-282. DOI: 10.1016/j.jtte.2016.05.005.

8. Vincent, L., Soille, P. Watersheds In Digital spaces: An Efficient Algorithm Based On Immersion simulation. *IEEE Trans. On Pattern Analysis And*

Machine Intelligence, 1991, vol. 13, iss. 6, pp. 583-598. DOI: 10.1109/34.87344.

9. Wang, D. A Multiscale Gradient Algorithm For Image Segmentation Using Watersheds. *Pattern Recognition*, 1997, vol. 30, iss. 12, pp. 2043-2052. DOI: 10.1016/S0031-3203(97)00015-0.

10. Shen, J., Lin, X., Shi, Y., Wong, C. Knowledge-Based Road Extraction From High Resolution Remotely Sensed Imagery. *IEEE Congress on Image and Signal Processing*, 2008, pp. 608-612. DOI: 10.1109/CISP.2008.519.

11. Bakhtiari, H. R. R., Abdollahi, A., Rezaeian, H. Semi Automatic Road Extraction From Digital Images. *The Egypt. J. Remote Sensing and Space Science*, 2017, vol. 20, iss. 1, pp. 117-123. DOI: 10.1016/j.ejrs.2017.03.001.

12. Xu, G., Zhang, D., Li, X. Road Extraction In High Resolution Images From Google Earth. *7th International Conference on Information, Communications and Signal Processing*, China, 2009, pp. 1-5. DOI: 10.1109/ICICS.2009.5397470.

13. Anil, P.N., Natarajan, S. A Novel Approach Using Active Contour Model For Semi-Automatic Road Extraction From High Resolution Satellite Imagery. *Second International Conference On Machine Learning And Computing*, 2010, pp. 263-266. DOI: 10.1109/ICMLC.2010.36.

14. Liu, Y., Yao, J., Lu, X., Xia, M., Wang, X., Liu, Y. RoadNet: Learning To Comprehensively Analyze Road Networks In Complex Urban Scenes From High-Resolution Remotely Sensed Images. *IEEE Trans. Geosci. Remote Sens.*, 2019, vol. 57, no. 4, pp. 2043-2056. DOI: 10.1109/TGRS.2018.2870871.

15. Lukin, V., Proskura, G., Vasilieva, I. Comparison Of Algorithms For Controlled Pixel-By-Pixel Classification Of Noisy Multichannel Images. *Radioelectronic And Computer Systems*, 2019, no. 4, pp. 39-46. DOI: 10.32620/reks.2019.4.04.

16. Ghasemloo, N., Mobasheri, M. R., Zare, A. M., Eftekhari, M. M. Road And Tunnel Extraction From SPOT Satellite Images Using Neural Networks. *Journal of Geographic Information System*, 2013, vol. 5, iss. 1, pp. 69-74. DOI: 10.4236/jgis.2013.51007.

17. Alshehhi, R., Marpu, P. R., Woon, W. L., Mura, M. D. Simultaneous Extraction Of Roads And Buildings In Remote Sensing Imagery With Convolutional Neural Networks. *ISPRS Journal of Photogrammetry And Remote Sensing*, 2017, vol. 130, pp. 139-149. DOI: 10.1016/j.isprsjprs.2017.05.002.

18. Xin, J., Zhang, X., Zhang, Z., Fang, W. Road Extraction of High-Resolution Remote Sensing Images Derived From DenseUNet. *Remote Sensing*, 2019, vol. 11, iss. 21, article no. 2499. DOI: 10.3390/rs11212499.

19. Zhang, Z., Liu, Q., Wang, Y. Road Extraction By Deep Residual UNet. *IEEE Geosci. Remote Sens.*

Lett., 2018, vol. 15, no. 5, pp. 749-753. DOI: 10.48550/arXiv.1711.10684.

20. Ronneberger, O., Fischer, P., Brox, T. UNet: Convolutional networks for biomedical image segmentation. *Computer Vision and Pattern Recognition*, 2015, pp. 1-8. DOI: 10.48550/arXiv.1505.04597.

21. *Massachusetts dataset*. Available at: https://www.cs.toronto.edu/~vmnih/data/mass_roads/train/sat/index.html (accessed on July 2021).

22. Shorten, C. C., Khoshgoufar, M. T. A Survey on Image Data Augmentation for Deep Learning. *J. Big Data*, 2019, vol. 6, article no. 60. DOI: 10.1186/s40537-019-0197-0.

23. Jiang, Y. Research on road extraction of remote sensing image based on convolutional neural network. *EURASIP Journal on Image and Video Processing*, 2019, article no. 31. DOI: 10.1186/s13640-019-0426-7.

24. Barbedo, J. G. A. Impact of dataset size and variety on the effectiveness of deep learning and transfer learning for plant disease classification. *Computers and Electronics in Agriculture*, 2018, vol. 153, pp. 46-53. DOI: 10.1016/j.compag.2018.08.013.

25. Yadav, S., Jadhav, S. M. Deep convolutional neural network based medical image classification for disease diagnosis. *Journal of Big Data*, 2019, vol. 6, article no. 113. DOI: 10.1186/s40537-019-0276-2.

26. Krizhevsky, A., Sutskever, I., Hinton, G. E. ImageNet Classification with Deep Convolutional Neural Networks. *Communications of the ACM*, 2017, vol. 60, iss. 6, pp. 84-90. DOI: 10.1145/3065386.

27. Szegedy, C., Vanhoucke, V., Ioffe, J., Shlens, J., Wojna, Z. Rethinking the Inception Architecture for Computer Vision. *Computer Vision and Pattern Recognition*, 2015, pp. 1-10. DOI: 10.48550/arXiv.1512.00567.

28. Szegedy, C., Liu, W., Jia, Y., Sermanet, P., Reed, S., Anguelov, D., Erhan, D., Vanhoucke, V., Rabinovich, A. Going Deeper with Convolutions. *IEEE Conference on Computer Vision and Pattern Recognition (CVPR)*, 2015, pp. 1-9. DOI: 10.1109/CVPR.2015.7298594.

29. He, K., Zhang, X., Ren, S., Sun, J. Deep Residual Learning for Image Recognition. *Computer Vision and Pattern Recognition*, 2015, pp. 1-12. DOI: 10.48550/arXiv.1409.4842.

30. Yaloveha, V., Podorozhniak, A., Kuchuk, H. Convolutional neural network hyperparameter optimization applied to land cover classification. *Radioelectronic and computer systems*, 2022, no. 1, pp. 115-128. DOI: 10.32620/reks.2022.1.09.

31. He, K., Sun, J. Convolutional neural networks at constrained time cost. *IEEE Conference on Computer Vision and Pattern Recognition*, 2015, pp. 5353-5360. DOI: 10.1109/CVPR.2015.7299173.

32. Badrinarayanan, V., Kendall, A., Cipolla, R. SegNet: A Deep Convolutional Encoder-Decoder Architecture for Image Segmentation. *IEEE Transactions on Pattern Analysis and Machine Intelligence*, 2017, vol. 39, iss. 12, pp. 2481-2495. DOI: 10.1109/TPAMI.2016.2644615.

33. Canziani, A., Paszke, A., Culurciello, E. An Analysis of Deep Neural Network Models for Practical Applications. *Computer Vision and Pattern Recognition*, 2016, pp. 1-7. DOI: 10.48550/arXiv.1605.07678.

Надійшла до редакції 1.07.2022 розглянута на редколегії 25.08.2022

**НОВИЙ ПІДХІД ДО СЕМАНТИЧНОЇ СЕГМЕНТАЦІЇ
АВТОМАТИЧНО ВИЛУЧЕНИХ ДОРОЖНІХ МЕРЕЖ З ЗОБРАЖЕНЬ
ДИСТАНЦІЙНОГО ЗОНДУВАННЯ ЗА ДОПОМОГОЮ МОДИФІКОВАНОЇ UNET**

*Мірал Дж. Патель, Ашіш М. Котарі,
Хасмух П. Корінга*

Точні й актуальні дорожні карти мають вирішальне значення для великої кількості застосувань, таких як міське планування, автоматична система навігації транспортних засобів і система моніторингу дорожнього руху. Однак навіть на зображеннях дистанційного зондування з високою роздільною здатністю фон і дороги виглядають схожими через оклюзію дерев і будівель, тому важко точно сегментувати дорожню мережу зі складних фонових зображень. У цій дослідницькій статті було запропоновано алгоритм, заснований на глибокому навчанні, для сегментації дорожньої мережі із зображень дистанційного зондування. Цей алгоритм семантичної сегментації було розроблено з модифікованою UNet. Через меншу доступність зображень дистанційного зондування для семантичної сегментації використовувався метод доповнення даних. Спочатку мережа семантичної сегментації була навчена більшою кількістю навчальних зразків з використанням традиційної архітектури UNet. Після цього кількість навчальних зразків поступово зменшується та вимірюється продуктивність традиційної моделі UNet. Ця базова модель UNet дає кращий результат у вигляді точності, IOU, оцінки DICE та візуалізації зображення для 362 навчальних зразків. Ідея полягає в тому, щоб просто отримати дані про дороги із зображень дистанційного зондування. Як наслідок, на відміну від традиційної UNet, немає потреби в глибокій структурі декодера нейронної мережі. Отже, кількість згорткових шарів у модифікованій UNet менша, ніж у стандартній UNet. Таким чином, було зменшено складність архітектури глибокого навчання та час навчання, необхідний для моделі дорожньої мережі. Продуктивність моделі, виміряна за допомогою об'єднання (IOU), становила 93,71%, а середній час сегментації одного зображення становив 0,28 секунди. Результати показали, що модифікована UNet може ефективно сегментувати дорожню мережу на основі зображень дистанційного зондування з ідентичним фоном. Її можна використовувати в різних ситуаціях.

Ключові слова: семантична сегментація; UNet; RoadNetwork; Extraction; модифікований UNet.

Мірал Дж. Пател – наук. співроб. каф. електроніки та зв'язку, Університет Атія; доц., Державний інженерний коледж, Раджкот, Гуджарат, Індія.

Ашіш М. Котарі – проф., зав. каф. електроніки та зв'язку, Університет Атія, Раджкот, Гуджарат, Індія.

Хасмух П. Корінга – доц. каф. електроніки та зв'язку, Державний інженерний коледж, Раджкот, Гуджарат, Індія

Miral J. Patel – Research Scholar of Electronics and Communication Department, Atmiya University; Assistant Professor, Government Engineering College, Rajkot, Gujarat, India, e-mail: mjpatelegc@gmail.com, ORCID: 0000-0003-0047-9552.

Ashish M. Kothari – Professor, Head of Electronics and Communication Department, Atmiya University, Rajkot, Gujarat, India, e-mail: amkothari.ec@gmail.com, ORCID: 0000-0002-1981-8465.

Hasmukh P. Koringa – Assistant Professor of Electronics and Communication Department, Government Engineering College, Rajkot, Gujarat, India, e-mail: hasmukh_meec@rediffmail.com, ORCID: 0000-0002-2521-3972.